

Modeling Cell-to-Cell Stochastic Variability in Intrinsic Apoptosis Pathway

Hsu Kiang Ooi and Lan Ma, *Member, EMBS*.

Abstract—Apoptosis is a cell suicide mechanism that enables metazoans to control cell number in tissues and to eliminate individual cells that threaten the animal's survival. Dependent on the type of stimulus, apoptosis can be propagated by intrinsic pathway or extrinsic pathway. Previously, we have proposed a deterministic model of intrinsic apoptosis pathway which is bistable in a robust parameter region. Cellular networks, however, are inherently stochastic and significant cell-to-cell variability in apoptosis response has been observed at single cell level. In this work, we examine the impact of intrinsic stochastic fluctuations as well as variation of protein concentrations on behavior of the intrinsic apoptosis network. First, Gillespie Stochastic Simulation Algorithm (SSA) of the model is implemented to account for intrinsic noise. Using histograms of steady-state output at varying input levels, we show that the intrinsic noise in the apoptosis network elicits a wider region of bistability. We further analyze the dependence of system stochasticity due to intrinsic fluctuations, such as steady-state noise level and random response delay time, on the input signal. We find however that the intrinsic noise is insufficient to generate significant stochastic variations at physiologically relevant level of molecular numbers. Finally, extrinsic fluctuation represented by variations of two key proteins is modeled and the resultant stochasticity of apoptosis timing is analyzed. Indeed, these protein variations can induce cell-to-cell stochastic variability at a quantitative level agreeing with experiments. Therefore, we conclude that the heterogeneity in intrinsic apoptosis responses among individual cells plausibly arises from extrinsic rather than intrinsic origin of fluctuations.

I. INTRODUCTION

The regulation of cells through apoptosis (programmed cell death) is a critical biological process involved in normal development as well as stress responses of multicellular organisms [1]. Apoptosis maintains a balanced number of cells and thus homeostasis. Excessive apoptosis leads to atrophy conditions such as neurodegenerative diseases while the failure to trigger apoptosis causes accumulation of dangerous cells and increased risk of tumor development. Apoptosis is mediated by two interconnected signaling pathways: the extrinsic pathway, activated in response to binding of extracellular ligands to death receptor, and the intrinsic pathway, initiated by intracellular death-inducing stimulus (hypoxia, DNA damage, etc.) [2]. Both pathways employ cascades of caspases, a family of intracellular cysteine proteases, to execute final cell death [3].

There have been considerable efforts in mathematical modeling and analysis of the biochemical network of extrinsic apoptosis, whereas the intrinsic apoptosis pathway has received less attention [5-7]. Based on the Fusseneger model

[8], we have developed a deterministic model of intrinsic apoptosis pathway (Fig. 1) governed by ordinary differential equations (ODEs), where the intrinsic caspase activation pathway and an additional positive feedback are incorporated [8]. We have shown previously that the steady-state response of the deterministic model exhibits bistability with a robust parameter region [8]. In this study, we examine the impact of stochastic variations on behavior of intrinsic apoptosis pathway, aiming to elucidate the plausible sources of the significant cell-to-cell variability in apoptosis response observed at single cell level recently [9]. We start with simulations of the model with intrinsic fluctuations, which is introduced by biochemical processes with low reactant numbers [10]. Standard Gillespie SSA of our model is implemented to account for intrinsic fluctuations in biochemical reactions [11]. The resultant bistability region expands as compared to the deterministic model due to intrinsic noise. Other system stochasticity due to intrinsic fluctuations, such as steady-state noise level and varying response delay time, are computed and their dependence on input signals is analyzed. We find that the intrinsic noise is insufficient to generate the observed cell-to-cell variations at physiologically relevant level of molecular numbers. Next, extrinsic noise represented by variations of two key apoptosis proteins, Cytochrome C protein (CC) and inhibitors of apoptosis (IAP), is integrated into the deterministic model and the resultant stochasticity are analyzed. Our simulations show that significant variability of the timing of intrinsic apoptosis response at single cell level can be induced by the variations of both proteins with a quantitative level comparable to experimental measurements.

II. RESULTS

A. Deterministic Model of Intrinsic Apoptosis Pathway

Our deterministic model of intrinsic apoptosis pathway is briefly reviewed here. The reaction scheme shown in Fig. 1 includes the core caspase cascade of intrinsic apoptosis. The pathway is initiated by the permeabilization of the mitochondria and the subsequent release of Cytochrome C (CC) that leads to a cascade of caspase activation. CC then binds to apoptotic protease-activator protein-1 (Apaf-1), forming a complex termed apoptosome. The binding with apoptosome transforms Pro-caspase 9 (c9p), precursor of active caspase, to its active form, Caspase-9 (c9a). The executioner pro-caspase (c3p) is activated by c9a to form active executioner caspase (CEA) through a process called proteolysis. CEA then cleaves vital cellular proteins and other caspases, driving the irreversible apoptosis process. An experimentally suggested positive feedback from CEA to c9a is included, which induces bistability of the model [12]. Finally CEA is subject to inhibition by IAP [7].

H.K. Ooi and L. Ma are with the Department of Bioengineering, University of Texas at Dallas, Richardson, 75080 TX, USA (corresponding author e-mail: lan.ma@utdallas.edu).

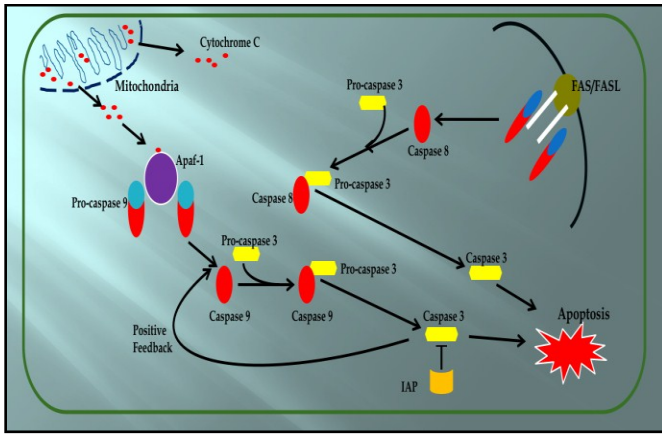


Figure 1. Intrinsic apoptosis model describes the activation of caspase cascade by the release of Cytochrome-C from the mitochondria.

Our deterministic model is represented by five interconnected ODEs, which are mostly adopted from the Fussenegger model except for the positive feedback loop [7]. An instance of interconnectivity is the coupling of $a1cc$ in equation (1) with equations (2) and (3). Note that all the binding and unbinding processes are represented by Michaelis-Menten kinetics under the quasi-steady-state assumption, where K_i ($i = H, K, L, P, U$) are the associated equilibrium constants of the binding processes. The formation of the complex Apoptosome is represented in equation (1). The binding process of CC to Apaf-1 occurs at a rate constant of k_{f1} . This complex dissociates at a rate constant of k_{r1} and the complex is degraded at a rate constant of μ_3 .

$$\frac{d[a1cc]}{dt} = \frac{k_{f1}[cc]}{1+K_H[cc]} - \frac{k_{r1}[a1cc]}{K_H} - \mu_3[a1cc] \quad (1)$$

Next, Apoptosome binds to Pro-caspase 9 ($c9p$) for activation. This is modeled by equation (2), where $c9p$ is constantly synthesized with a rate of Ω_9 , converted to caspase-9 ($c9a$) with a rate constant of k_{f2} and degraded with a rate constant of μ_4 .

$$\frac{d[c9p]}{dt} = \Omega_9 - \frac{k_{f2}[CEA]}{[CEA]+HC} \cdot \frac{[c9a] \cdot [a1cc] \cdot [c9p]^2}{\frac{1}{K_K \cdot K_L} + \frac{[c9p]}{K_L} + [c9p]^2} - \mu_4[c9p] \quad (2)$$

Once activated, $c9a$ shown in equation (3) is produced from $c9p$ with a rate constant of k_{f2} and degraded with a rate constant of μ_5 . The positive feedback introduced is a Hill function with a Hill Constant (HC) and a Hill coefficient of 1, shown in equations (2) and (3).

$$\frac{d[c9a]}{dt} = \frac{k_{f2}[CEA]}{[CEA]+HC} \cdot \frac{[c9a] \cdot [a1cc] \cdot [c9p]^2}{\frac{1}{K_K \cdot K_L} + \frac{[c9p]}{K_L} + [c9p]^2} - \mu_5[c9a] \quad (3)$$

The executioner pro-caspase ($c3p$) is expressed at a constant synthesis rate of Ω_{EZ} , activated to become executioner caspase $c3a$ (CEA) by $c9a$ with a rate constant of k_{f3} , and degraded with a rate constant of μ_6 in equation (4).

$$\frac{d[c3p]}{dt} = \Omega_{EZ} - k_{f3} \frac{[c9a]^n \cdot [c3p]}{1 + K_p} - \mu_6 \cdot [c3p] \quad (4)$$

In equation (5), the activation of $c3a$ by $c9a$ is induced with cooperativity $n=1.5$. CEA is degraded with a rate constant of μ_7 . IAP, assumed to have constant concentration in the deterministic model, degrades CEA following Michaelis-Menten kinetics with a rate constant of k_{su} .

$$\frac{d[CEA]}{dt} = k_{f3} \frac{[c9a]^n \cdot [c3p]}{1 + K_p} - \mu_7[CEA] - \frac{k_{su}[IAP][CEA]}{1+K_U[IAP]} \quad (5)$$

B. Stochastic Simulation of Intrinsic Noise

There has been extensive study of stochastic extrinsic apoptosis pathway [4, 13-14]. To investigate the influence of stochastic fluctuations on intrinsic apoptosis network, we apply the standard Gillespie SSA to our model accounting for the intrinsic noise. Specifically, the model is decomposed into 12 reaction (Rn) steps corresponding to the 12 elementary biochemical reactions (Table 1): Rn 1,2,3 (for apoptosome), Rn 4,5,6 (for $c9p$), Rn 5,7 (for $c9a$), Rn 8,9,10 (for $c3p$) and Rn 9,11,12 (for CEA). The decomposition step is done by identifying the molecular increment or decrement for each term in every ODE and assigning the identified terms to its corresponding elementary reaction. Each step is assigned with a reaction-occurrence probability and a random time interval for the next reaction, both dependent on its deterministic reaction rate (propensity function) [11]. For each iteration, SSA stochastically determines the next reaction and the time interval for the next reaction. The algorithm updates the numbers of molecules for each reacting species and the probability of each reaction at every iteration.

Table 1. Elementary reactions of the stochastic model denoted by their corresponding propensity functions (PF).

Reaction Number	Elementary Reaction PF	Reaction Number	Elementary Reaction PF
Rn 1	$\frac{k_{f1}[cc]}{1+KH[cc]}$	Rn 6	$\mu_4[c9p]$
Rn 2	$\frac{k_{r1}[a1cc]}{KH}$	Rn 7	$\mu_5[c9a]$
Rn 3	$\mu_3[a1cc]$	Rn 8	Ω_{EZ}
Rn 4	Ω_9	Rn 9	$\frac{k_{f3}[c9a]^n [c3p]}{\frac{1}{K_P} + [c3p]}$
Rn 5	$\frac{k_{f2}[CEA]}{[CEA]+0.1} \cdot \frac{[c9a] \cdot [a1cc] \cdot [c9p]^2}{\frac{1}{K_K \cdot K_L} + \frac{[c9p]}{K_L} + [c9p]^2}$	Rn 10	$\mu_6[c3p]$
		Rn 11	$\mu_7[CEA]$
		Rn 12	$\frac{k_{su}[IAP][CEA]}{1+KU[IAP]}$

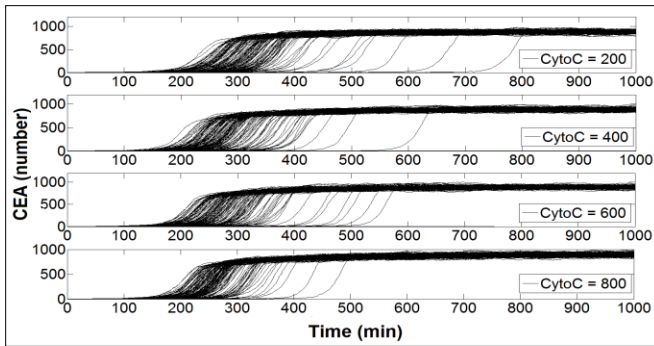


Figure 2. 150 time trajectories of CEA, representing apoptosis response in 150 cells are plotted at different CC values. The amount of time taken to activate CEA has less variability at high CC (i.e. 800) than at low CC (i.e. 200).

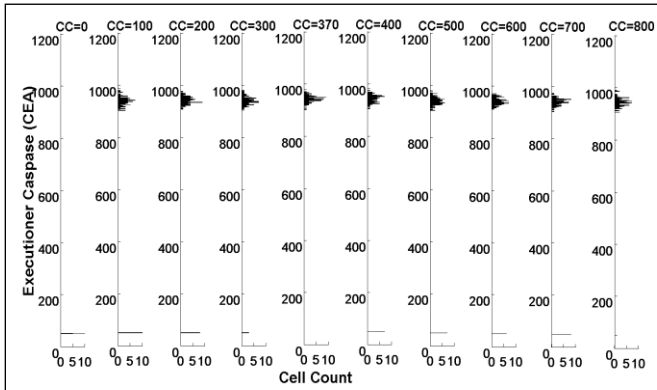


Figure 3. Histogram of steady-state CEA response. Bimodal distribution exists around two steady states, one at CEA=950 (High Steady State) and the other at CEA=20 (Low Steady State). The bimodal distribution implies bistability in the system. Bistability persists for the number of CC molecules in [20, 800].

Each run of stochastic simulation represents response in a single cell. A sample size of 150 cells is used. All the computations are implemented in MATLAB (Mathworks) and run on a 96-node computer cluster.

To model the effect of intrinsic noise, we first assume that the number of each reacting species involved in the intrinsic apoptosis pathway is below 1000 in an individual cell. Plotted in Fig. 2 are the 150 stochastic time trajectories of the output CEA response under varying numbers of Cytochrome C input. Each of the activation curve of CEA exhibits sigmoid shape, converging to an elevated steady state. In addition, there exists cell-to-cell variability in terms of the timing of CEA activation in that CEA in some cells is switched on later than other cells and higher number of CC induces less timing variability, consistent with experimental measurements of apoptosis dynamics [9]. To see if bistability holds for intrinsic apoptosis under intrinsic noise, histograms of the steady state of CEA (150 cells), under varying amount of input signal CC, is plotted in Fig. 3. We assume that bistability exists if the histogram presents bimodal distribution. Fig. 3 shows that bistability exists when the number of CC is greater than 20 (data not shown) and it persists till CC=800, indicating that the fold change of bistability region under intrinsic noise is above 4 times that of the deterministic model (where bistability region of CC = [0.08, 0.83] (nM) [8]). Such phenomenon of enhanced robustness induced by intrinsic noise supports

previous computational work which suggests that stochastic signaling networks may perform more robustly than their deterministic counterpart.

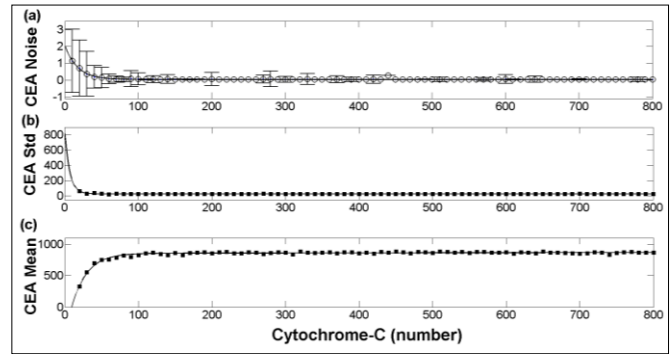


Figure 4. (a) Mean noise level (circle) of the steady-state CEA response, with error bars indicating the standard deviation. Noise is calculated as the ratio of standard deviation of CEA (b) over mean of CEA (c) at steady state, where the simulated results (solid squares) is fitted by dashed curves.

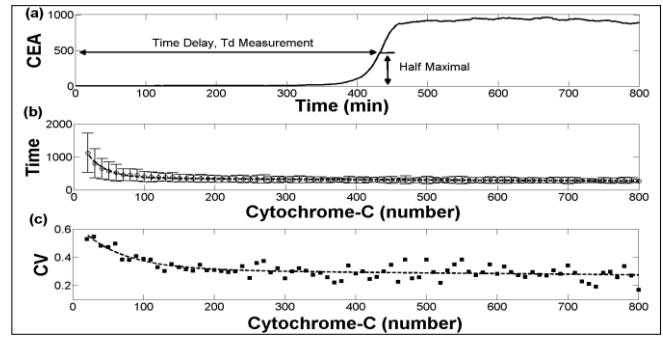


Figure 5. (a) T_d is the time it takes to reach half maximal of the steady-state CEA. (b) Mean delay time, T_d (black dots), as a function of CC. At low CC concentration, the standard deviation is larger (error bar). (c) Variance of T_d as a function of CC, where the simulated results (solid squares) is fitted by a dashed curve.

Next, statistics of the system stochasticity caused by intrinsic noise is evaluated. First, using the widely accepted definition of noise, namely the ratio of standard deviation over mean, we quantify the noise of the CEA output at steady state (Fig. 4). We find that at steady state the standard deviation of the stochastic CEA signal decreases while its mean value increases as the input signal CC increases (Fig. 4b, c). As a result, the mean noise of the output monotonically decreases and reaches minimum quickly with increasing amount of input (Fig. 4a). Secondly, each stochastic output time trajectory presents a delay time, T_d , between the input stimulation time ($t=0$) and the output activation time (half-max time) (Fig. 5a), consistent with experimental results [9, 15]. Statistics show that the mean value of T_d decreases with increasing CC level (Fig. 5b). In a population of 150 cells, the coefficient of variation (CV) of T_d decreases as CC increases (Fig. 5c), again agreeing well with experiments [9].

In order to simulate an accurate physiological condition of a cell, the number of molecules are increased to >10,000 [9]. Shown in Fig. 6, simulations with higher number of molecules suppresses the noise level to a negligible CV (~ 0.01), indicating that intrinsic noise is not sufficient to induce the observed stochasticity (CV ~ 0.15 -0.25) [9].

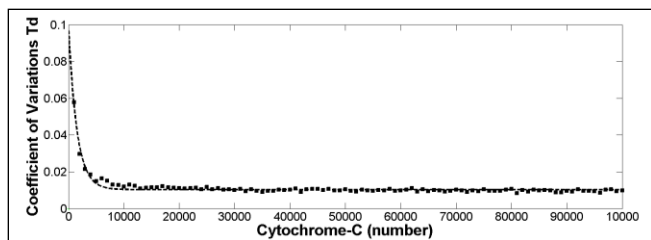


Figure 6. Coefficient of variation of the Time Delay, T_d , of CEA activation vs the number of CC molecules. The variability approaches a negligible CV values when the CC approaches 10,000 molecules. ■

C. Simulations of Protein Variations (Extrinsic Noise) and Combined Intrinsic & Extrinsic Noise.

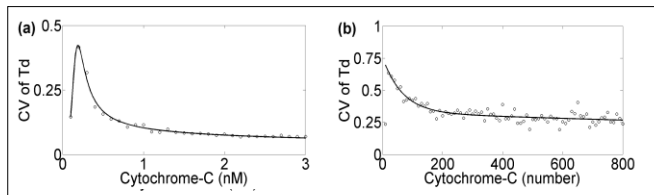


Figure 7. Mean value of Cytochrome C concentration is log-normally distributed with $CV = 0.25$. (a) CV of T_d for extrinsic noise only model. (b) CV of T_d for intrinsic noise model combined with extrinsic noise.

The impact of protein variations, which has been suggested as the source of extrinsic fluctuations for apoptosis pathway [9], is evaluated next. First, to simulate the variation of input molecules among individual cells, we assume that the concentration of CC is a random number obeying log-normal distribution around its mean value and the CV of CC is assumed to be 0.25, mimicking what has been measured before [9]. Using our deterministic model but random CC, we simulate 150 cells and calculate the CV of T_d at varying mean value of CC (Fig. 7a). The CV of T_d attains a peak value of ~ 0.42 at $CC = 0.2$ nM and maintains above ~ 0.05 . In addition, such extrinsic noise is applied to the stochastic model in previous section, simulating cells under both intrinsic and extrinsic noise (Fig. 7b). The combined noise leads to higher cell-to-cell variability with CV of T_d above 0.25.

Next, we study the extrinsic noise due to variation of IAP, a critical inhibitor of apoptosis, again assuming a log-normal distribution of IAP with $CV=0.25$. In Fig. 8, CC is fixed at different levels while IAP is random around its mean value for the deterministic model. The 2D heat map of the CV of T_d

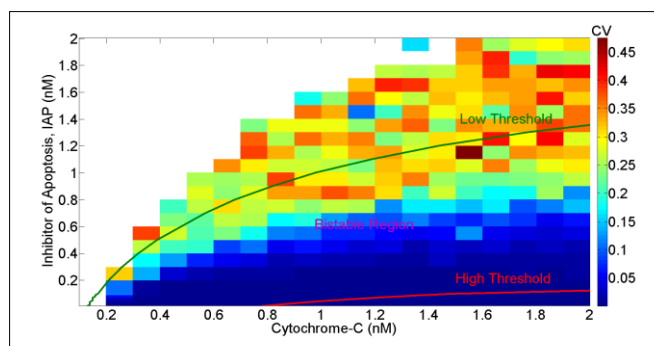


Figure 8. Coefficient of variation of the time delay, T_d , is shown as 2D heat map versus concentration of fixed CC & mean concentration of log-normally distributed random variable IAP. Superimposed are boundary curves of the deterministic bistability region with low (blue) and high (green) thresholds. Blank region means zero CV of T_d due to zero steady state of CEA.

shows that for the same CC concentration, increasing IAP will lead to higher variability in CEA activation. Comparing with the 2D bistability region, we find that the CV of T_d is highest (>0.2) around the low-CC-threshold curve of the bistability region. The above results show that the CV of T_d can achieve an experimentally measured level of ~ 0.2 under the variations of both proteins. Similar analysis is also done for the model with combined intrinsic and extrinsic noise. However, given the low numbers of protein molecules used (< 800), the random effect introduced by intrinsic noise is too strong such that no pattern of CV of T_d due to extrinsic noise is discovered.

III. CONCLUSION

Through stochastic simulations and analysis of the intrinsic pathway of apoptosis, we find that under low number of reactant molecules the intrinsic noise can enhance bistability region. However, in a physiologically relevant case, the high number of molecules suppresses the intrinsic noise to a negligible level. Thus extrinsic noise becomes dominant stochastic factor for intrinsic apoptosis and simulations show that the variation of protein concentration can plausibly induce the experimentally observed cell-to-cell variability.

ACKNOWLEDGMENT

The authors are grateful for the Start-up Fund from the University of Texas at Dallas.

REFERENCE

- [1] RC Taylor, SP Cullen and SJ Martin. "Apoptosis: controlled demolition at the cellular level." *Nat Rev Mol Cell Biol.* 9(3):231-41. March 2008.
- [2] JE Chipuk and DR Green. "Dissecting p53-dependent Apoptosis". *Cell Death and Differentiation*, March 2006.
- [3] SJ Riedl and GS Salvesen. "The apoptosome: signaling platform of cell death." *Nature Review Molecular Cell Biol.* Vol. 8 May 2007.
- [4] J Albeck, J Burke, S Spencer, DA Lauffenburger, PK Sorger. "Modeling a snap-action, variable-delay switch controlling extrinsic cell death." *PLoS Biol.* 6(12):2831-52. Dec 2008.
- [5] T Eissing, H Conzelmann, ED Gilles, F Allogowert, E Bullinger and P Scheurich. "Bistability Analyses of a Caspase Activation Model for Receptor-Induced Apoptosis." *Journal of Biol. Chem.* Vol. 279 No. 35 August 2004.
- [6] KL Ho and HA Harrington. "Bistability in apoptosis by receptor clustering." *PLoS Comput Biol.* 6(10):e1000956. Oct 2010.
- [7] M Fussenegger, JE Bailey and J Varner. "A Mathematical Model of Caspase Function in Apoptosis." *Nature Biotech.* July 2000.
- [8] H.K. Ooi and L. Ma, "Modeling Apoptosis Signaling Network: Ultrasensitivity versus Bistability." in Proc. of 27th Southern Biomedical Engineering Conference, Arlington, Texas. April 2011.
- [9] SL Spencer, S Gaudet, JG Albeck, JM Burke and PK Sorger. "Non-genetic origins of cell-to-cell variability in TRAIL-induced apoptosis." *Nature.* Vol. 459, May 2009.
- [10] M Thattai and A Oudenaarden. "Intrinsic Noise in Gene Regulatory Networks." *PNAS*, 8614-8619. vol. 98, no.15. July 2001.
- [11] DT Gillespie, "Exact stochastic simulation of coupled chemical reactions." *J. Phys. Chem.* 81:2340-61. December 1977.
- [12] M Creagh and SJ Martin. "Caspases: cellular demolition experts." *Biochemical Society Transactions.* Volume 29, pp 696-702, 2001.
- [13] T Eissing, F Allogowert and E Bullinger. "Robustness Properties of Apoptosis Models with Respect to Parameter Variations and Intrinsic Noise." *IEEE Proc. Syst. Biol.* Vol. 152, No. 4, December 2005.
- [14] Raychaudhuri S, Willgohe E, Nguyen TN, Khan EM, Goldkorn T. "Monte Carlo simulation of cell death signaling predicts large cell-to-cell stochastic fluctuations through the type 2 pathway of apoptosis." *Biophys J.* 2008 Oct;95(8):3559-62. Epub 2008 Jul 18.
- [15] SL Spencer and PK Sorger. "Measuring and modeling apoptosis in single cells." *Cell.* 2011 Mar 18;144(6):926-39.